Iranian Polymer Journal
**17** (9), 2008, 659-668

Available online at: http://journal.ippi.ac.ir

# Measurement of Thermal Transport Properties in Metal Doped Polypyrrole

Rashmi Saxena*, Vinodini Shaktawat, Kananbala Sharma, Narendra S Saxena*, and Thaneshwar P Sharma

Semi-conductor and Polymer Science Laboratory, University of Rajasthan
Jaipur-302004, India

Received 11 October 2007; accepted 6 September 2008

## A B S T R A C T

Simultaneous measurement of effective thermal conductivity ($\lambda_e$) and effective thermal diffusivity ($\chi_e$) of three samples of polypyrrole doped with metals Ni and Co in different percentage: polypyrrole doped with 100% Co (S1), polypyrrole doped with 50-50% Ni and Co (S2), and polypyrrole doped with 100% Ni (S3) have been made using transient plane source (TPS) technique. The amorphous nature of polypyrrole composites was confirmed by XRD studies. Characterization through SEM and EDX gives the information of surface morphology and elemental analysis of samples. From surface morphology it is found that surface is not smooth and contains macro-granular structure. EDX results confirm the presence of metal present in the samples. Thermal transport properties i.e., effective thermal conductivity ($\lambda_e$) and effective thermal diffusivity ($\chi_e$) were measured at normal pressure from room temperature to 170ºC. From these investigations, it has been found that both $\lambda_e$ and $\chi_e$ increase to maximum up to 110º and then a constant value is attained with further increase of temperature i.e., 170ºC. The values of $\lambda_e$ and $\chi_e$ of sample S3 doped with 100% Ni is higher as compared to sample S1 (Co 100%) and sample S2 (Ni, Co 50-50%). This result has been explained on the basis of bonding of cobalt and nickel with polypyrrole matrix during the polymerization and higher values for S3 are attributed to the more metallic nature of Ni.

**Key Words:**

composites;
conjugated polymers;
effective thermal conductivity;
effective thermal diffusivity;
metal halide.

## INTRODUCTION

In the last decade, the semiconducting and metallic properties of organic π-electron systems have drawn considerable attention both from fundamental and applications point of view [1] among various types of π-electron systems, the electrical optical and thermal properties of conjugated polymers have shown wide range of exciting features, leading towards applications like light emitting diodes, photodiodes, electronic circuits, lasers, sensors, solar cell, etc. After the discovery of conducting polymer, polyacetylene in 1977 [2], various π-conjugated systems, like polyaniline, polythiophene,

(*) To whom correspondence to be addressed.
E-mail: rashmi_saxena29@yahoo.co.in
N_S_Saxena@Rediff.com

poly(*para*)phenylene-vinylene, etc. have been prepared, and their physical properties have been investigated. Among the conducting polymers, polypyrrole (PPy) is promising for commercial applications because of its good environmental stability, facile synthesis and significant electrical conductivity than many other conducting polymers. PPy is easily prepared by either oxidative chemical polymerization or using electrochemical oxidation in aqueous or organic solutions by applying positive potential to a monomer solution containing an appropriate supporting electrolyte [3]. The oxidation of pyrrole, which involves the formation of radical anions and subsequent polymerization is given in Scheme I. PPy has an excellent thermal stability and it is a good candidate for use in carbon composites. Attempts have been made from time to time to investigate the thermal transport properties of polypyrrole [4-7] using different methods. Hosseini et al. [8], have reported thermal analysis and gas sensing behaviour by copolymer system with excellent thermal stability. Effects have also been made by Hosseini et al. [9], to prepare conducting fibres from cellulose and silk by PPy coating and to study their heat resistance. Ciuvasovaite et al. [10] have examined the possibility to apply a PANI-PPy blend coating for the gas chromatographic determination of parabens (*p*-hydroxybenzoates). New aspect of polyaniline doping using electrochemical quartz crystal nanobalance has been studied by Mirmohseni et al. [11]. Structural characteristics and thermal properties of poly(methyl methacrylate) are reported by Mohajery et al. [12]. Kaya et al. have investigated the thermal stability, conductivity and oligmor-metal complex [13]. Hashemi Doulabi et al. have reported the synthesis and characterization of biodegradable in situ forming hydrogels via direct polycondensation of poly(ethylene glycol) and fumaric acids [14]. In this paper macromers were synthesized through direct polycondensation technique and thermal characterization showed that the produced macromers have lower crystallinity than the original precursors. Thermal stability of poly(ether ether ketone) composites under dry-sliding friction and wear conditions presented by Fu et al. [15]. The results have shown that the PEEK composites exhibit stable friction coefficient and lower wear ratio.

However, very little effort has been made to understand, the heat energy dissipation through these polymeric materials. Since thermal parameters like thermal conductivity and thermal diffusivity at room temperature and elevated temperature play an important role in the selection of the material for fabricating devices for use at different temperatures, a study of $\lambda_e$ and $\chi_e$ at room as well as at elevated temperatures has been carried out.

**Material Preparation**

Metal halide composites of polypyrrole were prepared by oxidative polymerization of double distilled pyrrole using ammonium persulphate $(NH_4)\ S_2O_8$ as an oxidant. As a typical preparation sample S1 (Co=100%) was synthesized by taking ammonium persulphate (0.2 M) and metal halide (MX) monomer ratio (0.5 M) dissolved in HCl (1 M) pre-cooled to 0ºC. This aqueous solution was added to stirred solution. The temperature of this solution was maintained at 3-4ºC during mixing time. The black precipitate resulting from the reaction was washed with distilled water, methanol and then dried under vacuum for 6-8 h. Similarly sample S2 (Co=50% and Ni= 50%) and S3 (Ni=100%) were synthesized using the same procedure by varying the quantities of metal halides according to the stoichiometery. The polymer composites were ground in a mortar and pestle to obtain fine powder form. Pellets of thickness 2 mm and diameter 12 mm of these composites have been prepared using pressure machine at a load of 6 tons.

**Structural Characterization**

Structural characterization of these composites was

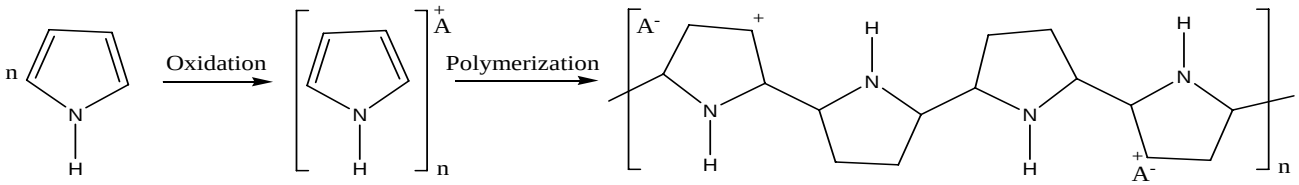


**Scheme I.** Oxidation of polypyrrole.

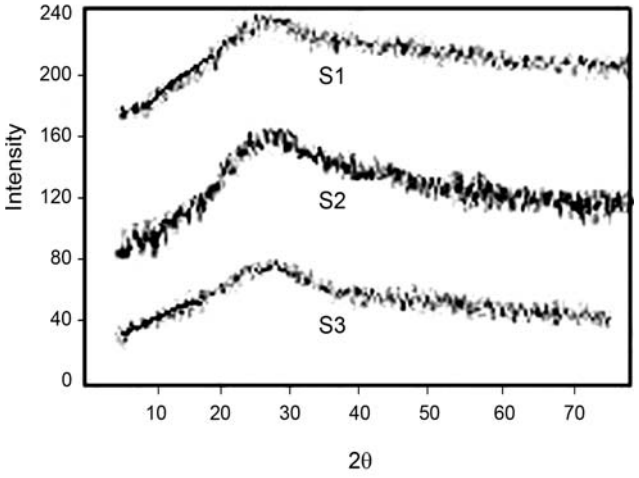


**Figure 1.** XRD of metal-doped polypyrrole.

carried out by X-Ray diffraction as shown through the diffraction pattern in Figure 1. The diffraction patterns of all samples show big hump at low diffraction angles, which confirm the amorphous nature of the polymer composites.

The morphology of PPy can be investigated using scanning electron microscopy (SEM). The wide range of magnification makes it suitable for investigation of microstructures and sometimes nanostructures of polymer. SEM also shows that the doping/dedoping process is often accompanied by major changes in morphology perhaps due to swelling caused by the insertion and removal of ions within the polymer matrix. With the help of SEM images, one can correlate the electrical conductivity, crystallinity, mechanical properties, etc. of polymer with its surface morphology. In the present study the effect of metal halide doping on the morphology and size is investigated. As each element of the periodic table has a unique electronic structure and, thus shows a unique response to electromagnetic waves. Such unique response gives characterization capabilities for each element in periodic table. So the chemical characterization (qualitative) is performed by energy dispersive X-ray fluorescence (EDX) analysis. In our study the SEM & EDX of all the samples were carried out using a SEM (Quanta Fe-200 model) attached to an EDX spectrophotometer. Gold coating was applied prior to recording the images. The images have same magnifications i.e., 3000 times. These SEM images are given in Figure 2. S1 (a), S2 (b), and S3(c) and elemental

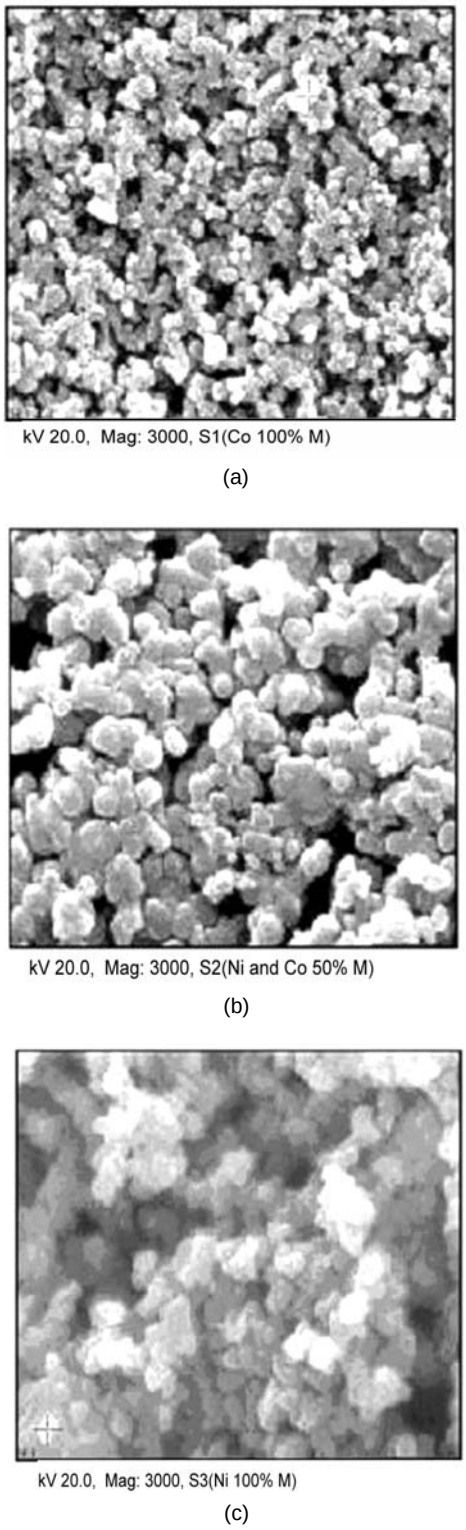


**Figure 2.** SEM image of S1 (a), S2 (b) and S3 (c).

analysis are also shown in Figure 3 [S1 (a), S2 (b), S3 (c)]. Tables 1-3 show elemental results, confirming the presence of metal doped in polypyrrole. It is clear that the structure is neither regular nor symmetric.

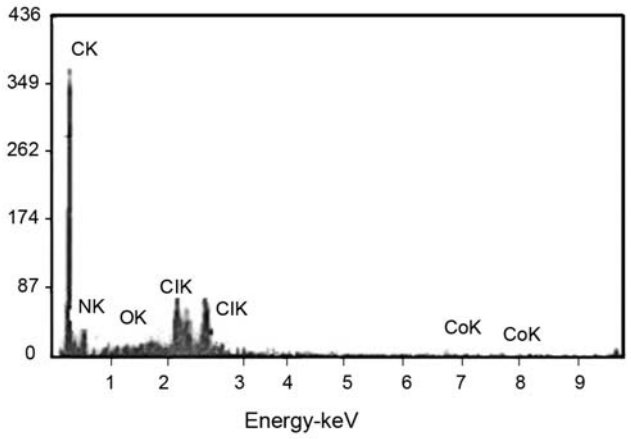


(a)

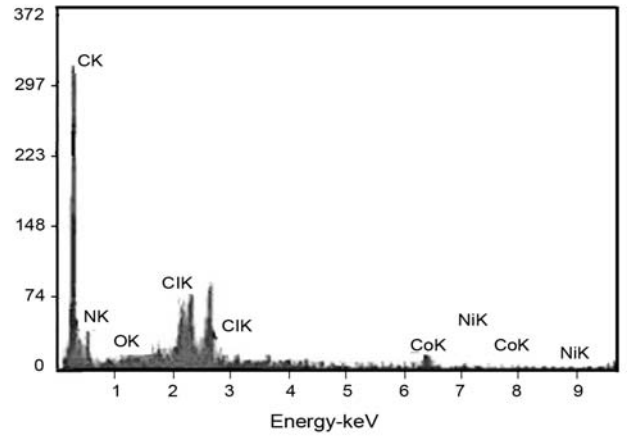


(b)

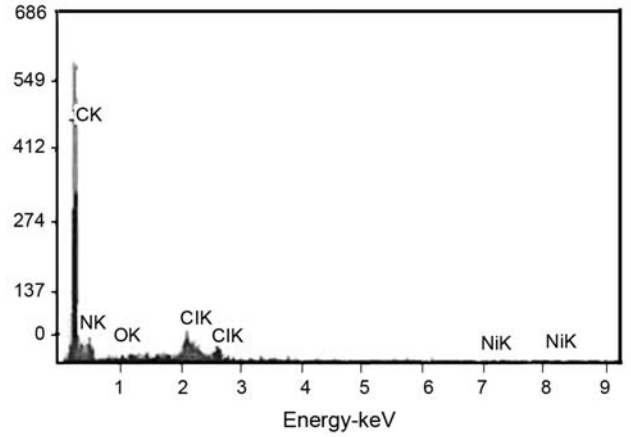


(c)

**Figure 3.** EDX patterns of S1 (a), S2 (b) and S2 (c).

The surface is not smooth and contains macro-granular structure formed by the aggregation of small globular structures. It is concluded from the SEM investigations that metal-doped polymer samples are non-fibrillar, and non-crystalline and the structure is similar to amorphous morphology. The EDX pattern of these metal halide doped polypyrrole composites is shown in Figure 3 while the elemental analysis is given in Tables 1-3. All the three samples, on which SEM was recorded, show traces of metal present in the sample. This clearly indicates that metal has been doped in the polymers. However, the presence of metal is very small. Due to such small atomic percentages of metals the XRD is unable to detect the presence of metals in the samples. The presence of chlorine is due to metal chloride doping and as the oxidation was carried by ammonium peroxide sulphate $(NH_4)_2S_2O_8$), signs of oxygen is found in the EDAX pattern.

**Table 1.** Elemental analysis of sample S1.

| Element | Weight (%) | Atomic percentage |
|---|---|---|
| CK | 65.05 | 71.53 |
| NK | 18.01 | 17.00 |
| OK | 11.56 | 09.55 |
| ClK | 04.75 | 01.77 |
| CoK | 00.67 | 00.15 |
| Matrix | Correction | ZAF |

## Thermal Characterization

Effective thermal conductivity ($\lambda_e$) and diffusivity ($\chi_e$) of these composites were determined by transient plane source (TPS) method, which is an extension of the transient hot strip (THS) method introduced by Gustafsson [16]. During the experiment for achieving the isothermal conditions in the sample, a constant current pulse is passed through the heating element. The measurements reported in this paper

**Table 2.** Elemental analysis of sample S2.

| Element | Weight (%) | Atomic percentage |
|---|---|---|
| CK | 61.27 | 68.54 |
| NK | 18.67 | 17.91 |
| OK | 13.31 | 11.18 |
| ClK | 05.52 | 02.09 |
| CoK | 00.82 | 00.19 |
| NiK | 00.42 | 00.10 |
| Matrix | Correction | ZAF |

**Table 3.** Elemental analysis of sample S3.

| Element | Weight (%) | Atomic percentage |
|---|---|---|
| CK | 64.15 | 69.32 |
| NK | 21.18 | 19.62 |
| OK | 12.95 | 10.50 |
| ClK | 01.22 | 00.45 |
| NiK | 00.49 | 00.11 |
| Matrix | Correction | ZAF |

were performed with TPS element of the type shown in Figure 4 it is made of 10 μm (micrometer) thick nickel foil with an insulating layer made of 50 μm (micrometer) thick kapton, on each side of the metal pattern. Evaluation of these measurements was performed in a way that was outlined by Gustafsson [16]. No influence could be recorded from electrical connections, which are shown in Figure 5. These connecting leads had the same thickness as the metal pattern of the TPS elements. TPS element (sensor which is used during the experiment) has a resistance at room temperature at about 3.26 Ω and a temperature coefficient (TCR) of around $4.6\times10^{-3}$ $K^{-1}$. The TCR of the element is such that the temperature increases of the element can be precisely deduced from a recording of its resistance. This specification is given by the manufacturer of TPS [16]. Owing to the change in average temperature of the sensor, the potential difference across the terminals is recorded by a digital multimeter and the current through the TPS sensor with digital power supply. Figure 6 shows the sample holder containing these samples, which is placed in a furnace. The current in the circuit is adjusted according to the nature of the sample material. At least three sets of readings at appropriate intervals are taken to ensure the accuracy of the results. The TPS programme used

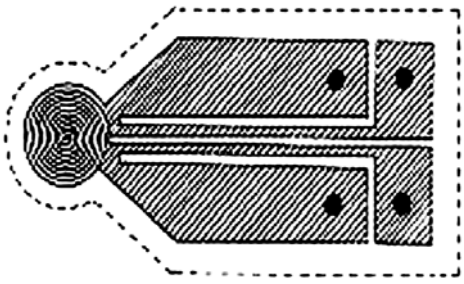

**Figure 4.** TPS sensor.

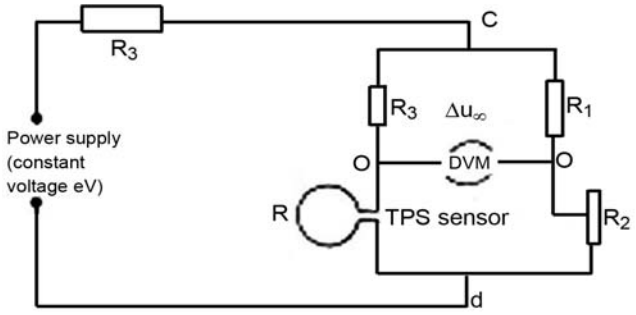


**Figure 5.** Bridge circuit.

here is capable of recording the temperature of the sample through the TPS sensor. In addition to this a sensitive thermometer is kept just above the sample pieces inside the furnace to monitor the temperature of the sample

**TPS Theory**

The TPS method consists of an electrically conducting pattern, which serves both as source of heat given to the material and as a sensor of temperature increase in the sample. Assuming the conducting pattern to be in y-z plane of a co-ordinate system, the rise in the temperature at a point y-z at time (t) due to an output power Q per unit area is given by Gustafsson [16].

$$DT(y,z,\tau) = \frac{1}{4\pi^{3/2}a\lambda}\int_0^{\tau}\frac{d\sigma}{\sigma^2}\int_A dy'dz'Q(y',z',t-\frac{\sigma^2a^2}{\chi})$$

$$\exp\left[\frac{-(y-y')^2-(z-z')^2}{4\sigma^2a^2}\right] \qquad (1)$$

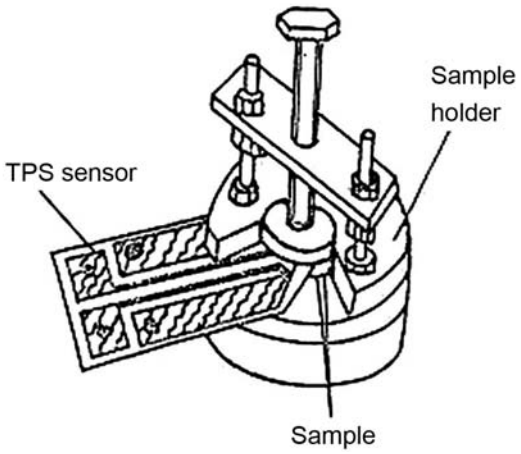


**Figure 6.** Sample holder.

where $\chi(t-t') = \sigma 2\ a^2$, $\theta = a^2 / \chi$, and $\tau = [t/\theta]^{1/2}$

$$\chi = \lambda/\rho C \quad (2)$$

where 'C' is the specific heat and '$\rho$' the density of material.

a is the radius of the hot disc (source and the sensor) which gives a measurement of the overall size of resistive pattern and $\theta$ is known as the characteristic time, $\sigma$ is a constant variable, $\lambda$ is the thermal conductivity in units of W/mK and $\chi$ is the thermal diffusivity in unit of $mm^2/s$ of the sample. The temperature increase $\Delta T$ (y, z, $\tau$) because of flow of current through the sensor gives rise to a change in the electrical resistance $\Delta R$ (t), which is given as

$$\Delta R(t) = \alpha \quad R_o \overline{\Delta T(\tau)} \quad (3)$$

where $R_o$ is resistance of TPS element before the transient recording has been initiated at room temperature, $\alpha$ is the temperature coefficient of resistance (TCR) and $\Delta T(\tau)$ is the properly calculated mean value of the time dependent temperature increase of the TPS element. $\Delta T(\tau)$ is calculated by averaging the increase in temperature of TPS element over the sampling time because the concentric ring sources in TPS element have different radii and are placed at different temperatures during the transient recording. During the transient event, $\Delta T(\tau)$ can be considered to be a function of time only, whereas, in general, it will depend on such parameters as the output power in TPS element, the design parameters [17] of the resistive pattern, and the thermal conductivity and thermal diffusivity of surroundings.

It is possible to write down an exact solution [16] for the hot disc if it is assumed that the disc contains a number 'm' of concentric rings as sources. From the ring source solution [18] we immediately have,

$$\overline{\Delta T(\tau)} = \frac{P_o}{\pi^{3/2} a \lambda} D_s(\tau) \quad (4)$$

where

$$D_s(\tau) = [m(m+1)]^{-2} \int_0^{\tau} \frac{d\sigma}{\sigma^2} \left[ \sum_{l=1}^{m} l \left\{ \sum_{k=1}^{m} k \exp \frac{-(l^2 + k^2)}{4\sigma^2 m^2} L_0 \left( \frac{lk}{4\sigma^2 m^2} \right) \right\} \right] \quad (5)$$

In eqn (4), $P_0$ is the total output power, $L_0$ is the modified Bessel function and l and k are the dimensions of the resistive pattern. To record the potential difference variations, which normally are of the order of a few millivolts during the transient recording, a simple bridge arrangement as shown in Figure 3 has been used. If we assume that the resistance increase will cause a potential difference variation $\Delta U(t)$ measured by the voltmeter in the bridge, the analysis of the bridge indicates that

$$\Delta E(t) = \frac{R_s}{R_s + R_o} I_o \Delta R(t) = \frac{R_s}{(R_s + R_o)} \frac{I_o \alpha R_o P_o}{\pi^{3/2} a \lambda} D_s(\tau) \quad (6)$$

where

$$\Delta E(t) = \Delta U(t)\ [1 - C.\ \Delta U(t)]^{-1} \quad (7)$$

and

$$C = \frac{1}{R_s I_o \left[ 1 + \frac{\gamma R_p}{\gamma(R_s + R_o) + R_p} \right]} \quad (8)$$

The definition of various resistances is given in Figure 3. $R_p$ is the lead resistance, $R_s$ is a standard resistance with a current rating that is much higher than $I_o$, which is the initial heating current through the arm of the bridge containing the TPS-element. $\gamma$ is the ratio of the resistances in two ratio arms of the bridge circuit, which is taken to be 100 in the present experiment. Determination of $\lambda$ and $\chi$ have been done using eqns (1) and (5), calculating $Ds(\tau)$ using a computer programme and recording the change in potential difference $\Delta U(t)$ it is possible to determine thermal conductivity $\lambda$. Thermal diffusivity $\chi$ can be determined by finding the value of characteristic time. The computer software installed in a PC was dedicated to these measurements.

## RESULTS AND DISCUSSION

XRD characterization suggests amorphous nature of the samples. SEM, EDX analyses give the morphological and doped elements confirmation in PPy matrix. Conjugated polymers may be doped just like inorganic semiconductors to become more conducting. The variation of effective thermal conductivity ($\lambda_e$) and thermal diffusivity ($\chi_e$) of the above-mentioned polypyrrole sample has been studied from room temperature i.e., 30ºC to 170ºC. The temperature of the heating furnace is mainted at the fixed temperature and then the data are recorded. In order to check the reproducibility of the results three experiments have been performed at each temperature and the results have been plotted in the error bar form for its principle value. The variation of these two thermal transport properties with temperature is shown in Figures 7a, 7b, 7c (effective thermal conductivity) and Figures 8a, 8b, 8c (effective thermal diffusivity). It is noticed that $\lambda_e$ and $\chi_e$ of each sample increases to maximum up to 110ºC and then it is constant with further increase of temperature i.e., up to 170ºC. The thermal conductivity is maximum for sample S3 (Ni=100 M%) and lowest conductivity is obtained for sample S2 (50-50% Ni-Co) whereas for sample S1 (Co=100 M%) the values of $\lambda_e$, $\chi_e$ lie in between S2 and S3. The glass transition temperature ($T_g$) of polypyrrole is 140ºC to 160ºC, but after doping the $T_g$ is shifted to 110ºC. This trend indicates that the $\lambda_e$ and $\chi_e$ of 100% Ni in the composites is higher over the values obtained in case of composites containing 100% Co. Electronic configurations of nickel (Z=28) and cobalt (Z=27) are [Ar] $3d^8 4s^2$ and [Ar] $3d^7 4s^2$. In polypyrrole matrix nitrogen has one lone pair electron and when metal is doped in the matrix, a bond formation between metal (Ni and Co) and nitrogen takes place [19]. This bond formation is responsible for the increased value of thermal conductivity of the composites (S1 and S2) doped with Ni and Co. It is interesting to note that bonding between Ni and nitrogen is as strong as compared to the bonding between Co and nitrogen of polypyrrole due to the more metallic character of Ni as compared Co. Improved bond strength between nitrogen and nickel in turn enhances the thermal transport properties as mentioned above. For sample S2 (Ni=50 M%, Co=50 M%), the probability

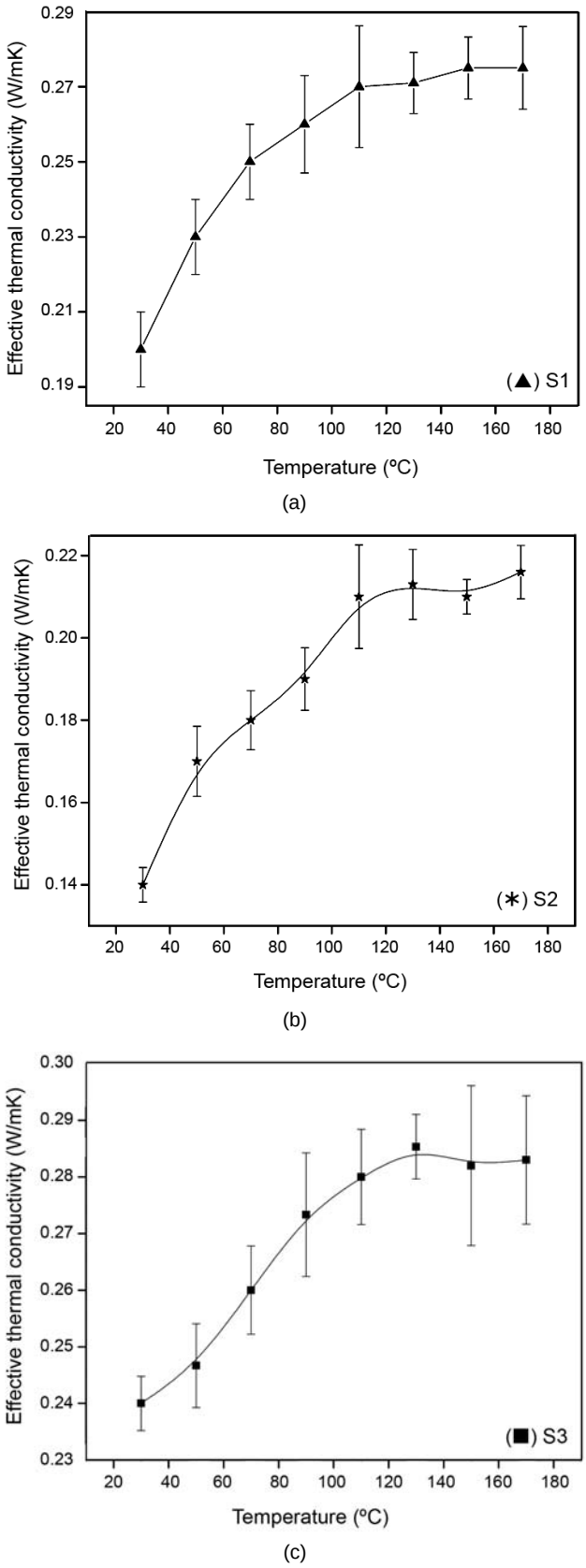


**Figure 7.** Effective thermal conductivities of S1 (a), S2 (b) and S3 (c).

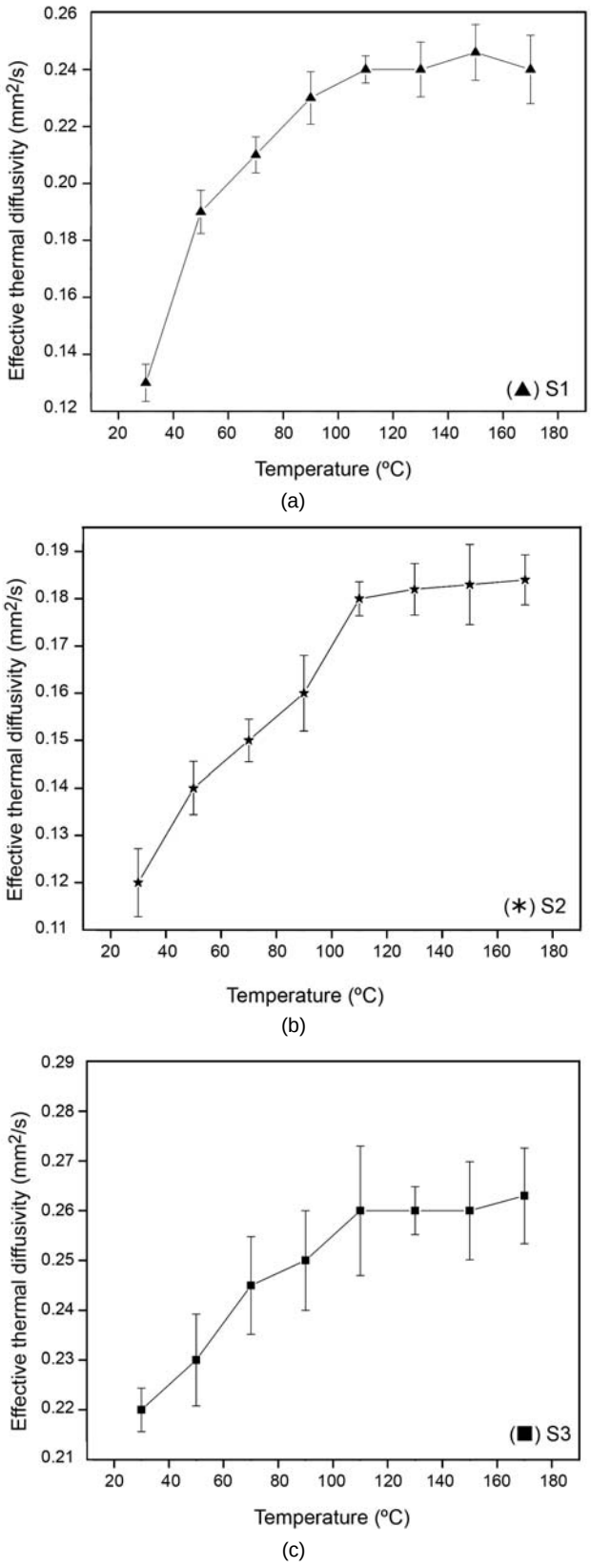


**Figure 8.** Effective thermal diffusivities of S1 (a), S2 (b) and S3 (c).

of formation of metallic bond between Ni and Co is much higher then the bond formation between metal (Ni and Co) and nitrogen of PPy matrix. When metal ion is doped in PPy matrix the metal ion is attached on polymer backbone as a counterion to ensure the overall charge neutrality. The imine (-NH=) group present in PPy is attached by Ni ion to make a bond formation. The same mechanism is followed for sample S1 (Co-100%) with Ni being more metallic then Co. Ni doped composite shows higher conductivity as compared to Co doped. In sample S2 there are two different types of metals (Ni and Co) doped with PPy, which make a metallic bond to produce some metal complexes. Metal complexes so formed create cluster in the sample and do not attach to the polymer backbone and act as scattering centres for the phonons and hence reduce the conductivity. Also polypyrrole shows a rougher and more porous surface morphology [20]. The linear but modest increase in the values of $\lambda_e$ & $\chi_e$ is due to the decrease in moisture contents of the samples with increase in temperature. The decrease in the moisture content in the sample increases the compactness of the sample [21] and as a result there is a decrease in the porosity. This enhances the process of thermal conduction and hence the thermal conductivity and diffusivity increases.

## CONCLUSION

In the present study, Ni and Co are doped at different concentrations in PPy matrix. XRD characterization suggests amorphous nature of the samples. SEM and EDX analyses give the morphological and doped elements confirmation in PPy matrix. Conjugated polymers may be doped just like inorganic semiconductors to become more conducting. The lowering of $T_g$ of the composite is indicative of the fact that metal doping produces loose structure in the sample. Ni doped PPy composites show higher value of thermal conductivity among all the samples (S1-S3), which is attributed to higher metallic character of Ni, whereas Ni-Co doped composites show the lowest thermal conductivity since they form metallic bond during the doping process. It can be concluded that single metal doped composite is better as compared to double metal doped composite. Systematic studies of effec-

tive thermal conductivity and effective thermal diffusivity of the mentioned conducting polymer in the temperature range from (room temperature) 30ºC to 170ºC is suggestive of the fact that these polymers are good for thermal applications in the range from 110ºC to 170ºC.

## ACKNOWLEDGEMENTS

Rashmi Saxena is thankful to Mr. N Jain, Mr. VK Saraswat, Mr. V Kishore, Mr. D Patidar, Miss Mansavi Dixit, and Miss Deepika Chaudhary who have helped in various ways during the course of this work.

## REFERENCES

1. Skatheim TA, Elsenbaumer RL, JR, *Handbook of Conducting Polymer*, Reynolds (Ed), 2nd ed, Marcel & Dekker, NY, 1998.
2. Heegeer AJ, Chian CK, Fincher CR, Park YW, Shirakawa H, Louis EJ, Gau SC, MacDiarmid AG, Synthesis of electrically conducting organic polymers-halogen derivatives of polyacetylene (ch)x, *J Chem Soc Chem Commun*, 578-580, 1977.
3. Wang LX, Li XG, Yang YL, Preparation, properties and applications of polypyrroles, *J React Funct Polym*, **47**, 125-139, 2001.
4. Lunn BA, Unsworth J, Booth NG, Ionis PC, Determination of the thermal conductivity of polypyrrole over the temperature range 280K-335K, *J Mater Sci*, **28**, 5092-5098, 1993.
5. Kim IW, Lee JY, Lee H, Solution-cast polypyrrole film-the electrical and thermal properties, *J Synth Met*, **78**, 177-180, 1996.
6. Ansari Khalkhali R, Effect of thermal treatment on electrical conductivities of polypyrrole conducting polymers, *Iran Polym J*, **13**, 53-60, 2004.
7. Ozdilek C, Hacaloglu J, Toppare L, Yagci Y, Structural and thermal characterization of PTSA doped polypyrrole-polytetrahydrofuran graft copolymer, *J Synth Met*, **140**, 69-78, 2004.
8. Hosseini SH, Entezami AA, Graft copolymer of polystyrene and polypyrrole and studies of its gas and vapour sensing properties, *Iran Polym J*, **14**, 101-110, 2005.
9. Hosseini SH, Pairovi A, Preparation of conducting fibres from cellulose and silk by polypyrrole coating, *Iran Polym J*, **14**, 934-940, 2005.
10. Ciuvasovaite V, Adomaviciute E, Vickaita V, Solid-phase micro extraction of parabens by polyaniline-polypyrrole coating, *CHEMIJA*, **18**, 11-15, 2007.
11. Mirmohseni A, Oladegaragoze A, Fotoohifar F, New aspects of polyaniline doping: a study based on using electrochemical quartz crystal nanobalance, *Iran Polym J*, **16**, 3-12, 2007.
12. Mohajery Sh, Entezami AA, Structural characteristics and thermal properties of poly(methyl methacrylate) and atactic polystyrene grafted onto metallocene based ethylene-allylbenzene copolymer, *Iran Polym J*, **16**, 345-355, 2007.
13. Kaya I, Koyuncu S, Thermal stability, conductivity and band gaps of oligo-2-[(phenylimino) methyl] phenol and oligomer-metal complex, *Iran Polym J*, **16**, 261-270, 2007.
14. Hashemi Doulabi AS, Sharifi S, Imani M, Mirzadeh H, Synthesis and characterization of biodegradable in situ forming hydrogels via direct polycondensation of poly(ethylene glycol) and fumaric acid, *Iran Polym J*, **17**, 125-133, 2008.
15. Fu H, Lio B, Wang YH, Xiao FR, Sun BC, Thermal stability of poly(ether ether ketone) composites under dry-sliding friction and wear conditions, *Iran Polym J*, **17**, 493-501, 2008.
16. Gustafsson SE, Transient plane source techniques for thermal conductivity and thermal diffusivity measurements of solid materials, *J Rev Sci Inst*, **62**, 797-804, 1991.
17. Gustafsson SE, Suleiman B, Saxena NS, Haq IU, The transient plane source technique experimental design criteria, *J High Temp High Press*, **23**, 289-293, 1991.
18. Carslaw H, Jaeger S, *Conduction of heat in solid*, Oxford University, CJ, 1959.
19. Joshi GP, Saxena NS, Sharma TP, Dixit V, Mishra SCK, Thermal transport in chemically doped polyaniline materials, *J Phys Chem Solid*, **64**, 2391-2396, 2003.
20. Liu YC, Tsai CJ, Enhancements in conductivity and thermal and conductive stabilities of electropolymerized polypyrrole with caprolactum-modi-

fied clay, *Chem Mater*, **15**, 320-326, 2003.
21. Shekeil A, Aghbari S, DC electrical conductivity of some poly(pyrrole-metal) complexes, *J Macromol Sci Part A Pure Appl Chem*, **41**, 649-667, 2004.